# Molecular Ultrasound Monitoring of Early Artery Injury After Carotid Balloon Angioplasty

Xinhai Mo[1], Fei Yan[2]* and Bo Zhang[1]*

[1] Department of Ultrasound in Medicine, Shanghai East Hospital, Tongji University School of Medicine, Shanghai, China,
[2] Paul C. Lauterbur Research Center for Biomedical Imaging, Institute of Biomedical and Health Engineering, Shenzhen Institutes of Advanced Technology, Chinese Academy of Sciences, Shenzhen, China

Cardiovascular intervention is a common treatment procedure for many cardiovascular diseases. But restenosis often occurs after these procedures, greatly discounting their long-term therapeutic effects. Early detection of endothelial denudation is helpful for the diagnosis and prevention of restenosis. Here, we fabricated targeted microbubbles by conjugating anti-collagen IV antibodies to the surface of biotinylated microbubbles ($MB_{ColIV}$) and applied them for ultrasound molecular imaging of endothelial injury at early stage. Our results showed that the $MB_{ColIV}$, with a typical multi-peak particle distribution, was successfully constructed, which was confirmed by Alexa Fluor® 555-labeled secondary antibody. *Ex vivo* adhesion of microbubbles revealed that $MB_{ColIV}$ can effectively and specially bind to the surface of balloon-injured carotid artery. The *in vivo* animal experiments showed ultrasound molecular imaging signals from carotid artery-injured rats administrated with $MB_{ColIV}$ were significantly higher than those administrated with isotype control microbubbles. Histological staining of the left carotid common artery revealed that collagen IV was obviously exposed after endothelium denudation in balloon-injured artery. In conclusion, our current study provides an effective approach to detect vascular injury at the early stage and a potential platform for image-guided therapy to vascular injury.

Keywords: ultrasound molecular imaging, collagen IV, artery injury, restenosis, targeted microbubbles

## INTRODUCTION

Cardiovascular diseases from atherosclerosis are responsible for the major cause of mortality worldwide (Murray et al., 2012). Pathologically, atherosclerosis is a chronic and progressive disease featured with retention of lipids, accumulation of extracellular matrix and infiltration of smooth muscle cells (SMCs) with or without macrophages (Otsuka et al., 2016). Due to atherosclerotic lesions, cardiovascular events often occur in a complex and unpredictable manner, resulting in a series of complications. Among these, stenosis and thrombosis are the two major complications. Stenosis may cause distal organ ischemia and thrombosis, and trigger thrombotic occlusion of artery to organs, ultimately resulting in life-threatening cardiovascular events.

Early invasive therapies, such as percutaneous coronary intervention (PCI), could improve long-term survival and reduce late myocardial infarction and recurrent unstable angina requiring rehospitalization for patients with non-ST-elevation myocardial infarction (Bavry et al., 2006; Amsterdam et al., 2014). Although the narrowed or obstructed arteries are recovered through

endovascular procedures, post-operational restenosis is generally inevitable. The main reason is that mechanical endovascular procedures often cause endothelial damage by activating a series of inflammatory pathways. Due to these inflammatory effects, excessive migration, and proliferation of SMCs, and plentiful synthesis and deposition of extracellular matrix lead to intimal hyperplasia. The serious intimal hyperplasia will result in restenosis which may represent a fatal threat for patients. Evidence demonstrated that restenosis occurs in up to 60% post-angioplasty patients within the first year because of mechanical vascular injury (Petrasheskaya et al., 2016). Therefore, early detection at the stage of endothelial denudation is desirable for the diagnosis and prevention of restenosis.

During vascular injury, many cell adhesion molecules are overexpressed or upregulated. Selectins, integrins, and the immunoglobulin superfamily of cell adhesion molecules are the three major classes of leukocyte cell adhesion molecules (Davis et al., 2003). Numerous studies have shown that intracellular adhesion molecules-1 (ICAM-1), vascular cell adhesion molecules-1 (VCAM-1) or P-selectin can serve as the targets for various imaging probes (Wu et al., 2011; Yan et al., 2018). However, these cell adhesion molecules are not expressed promptly during vascular injury. Generally, it takes 1 day, or even longer, to increase their expression on the surface of vascular endothelial cells (Tanaka et al., 1993; Kennedy et al., 2000).

Collagen IV, representing 50% of the vascular basement membrane, could be exposed immediately when the intact endothelial monolayer is denuded by mechanical injury of vascular intervention (Kalluri, 2003). That is, the expression of collagen IV is time-independent and related to endothelial denudation and damage. Therefore, collagen IV can be used as targeting receptor for detection, and even treatment at the site of vascular injury (Chan et al., 2011; Meyers et al., 2017).

Ultrasonography, a non-invasive and real-time imaging method, is widely used to examine cardiovascular diseases (Yan et al., 2018). With the help of targeted microbubbles (MBs), ultrasound molecular imaging allows to detect specific lesions at molecular level. Generally, the applications of ultrasound molecular imaging require the effective binding of ultrasonic probes to the receptors in the physiologic flow conditions after their intravenous administration. Antibodies, antibody fragments, peptides, and carbohydrates have been conjugated to the surface of MBs. By detecting the signals derived from retained MBs in the target regions, ultrasound molecular imaging can visualize molecular dynamics in situ. Currently, several stuieds have been published to demonstrate the diagnostic utility of ultrasound molecular imaging for the detection of inflammation, atherosclerosis and tumor angiogenesis (Villanueva and Wagner, 2008; Willmann et al., 2008; Leong-Poi, 2009; Lindner, 2009; Deshpande et al., 2010). In this study, we fabricated a novel targeted MBs by conjugating anti-collagen IV antibodies to the surface of biotinylated MBs (MB$_{Col IV}$) and applied them for ultrasound molecular imaging of endothelial injury at early stage (**Figure 1**).
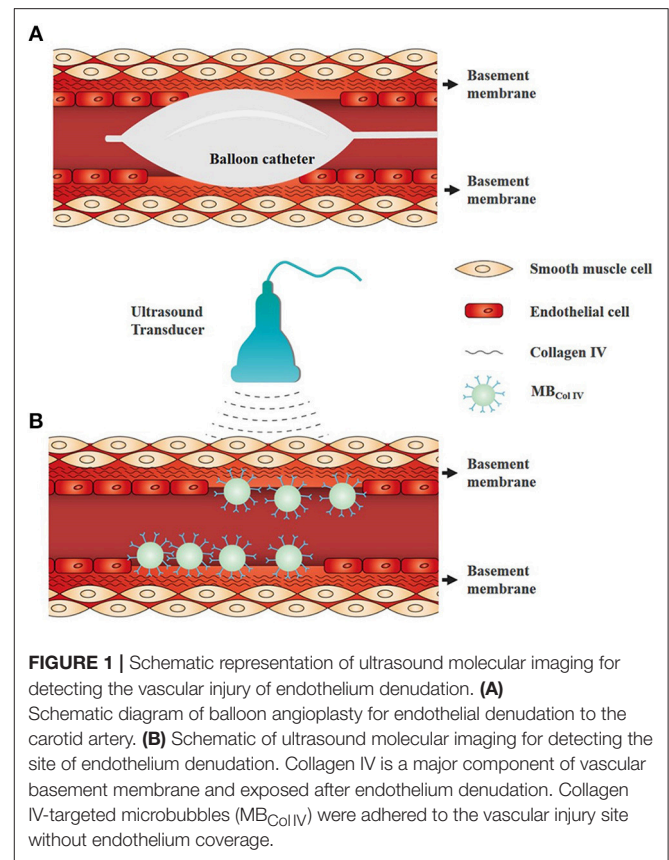


**FIGURE 1 |** Schematic representation of ultrasound molecular imaging for detecting the vascular injury of endothelium denudation. **(A)** Schematic diagram of balloon angioplasty for endothelial denudation to the carotid artery. **(B)** Schematic of ultrasound molecular imaging for detecting the site of endothelium denudation. Collagen IV is a major component of vascular basement membrane and exposed after endothelium denudation. Collagen IV-targeted microbubbles (MB$_{Col IV}$) were adhered to the vascular injury site without endothelium coverage.

## MATERIALS AND METHODS

### Preparation of MBs

Biotinylated, lipid-shelled MBs were prepared as previously described (Yan et al., 2013). Briefly, DSPC, DSPE–PEG2000 and DSPE–PEG2000-Biotin (Avanti Polar Lipids, Alabaster, AL, USA) (molar ratios = 9:0.5:0.5) were blended in chloroform. The solvent was evaporated under nitrogen flow at room temperature, forming a thin film on the wall of the test tube. Residual chloroform was further removed by vacuum treatment for at least 2 h. The completely dried phospholipid membrane was hydrated at 60°C with a given buffer consisting of 0.1 M Tris (pH 7.4):glycerol:propylene glycol (80:10:10 by volume), and then transferred into vials. After sealing the vials, the air in the vials was replaced with perfluoropropane ($C_3F_8$). Biotinylated MBs (MB$_{biotin}$) were obtained by mechanically vibrating for 30 s. The resulting MB$_{biotin}$ were washed with phosphate buffered saline (PBS) solution twice to eliminate excess unincorporated lipids by centrifuge at 400 g for 3 min. Three microgram of avidin per $10^7$ MBs was then incubated with the MB$_{biotin}$ dispersion for 30 min at room temperature, followed by rinsing three times to remove unreacted avidin (Aladdin, Pudong, Shanghai, China). Then either 2.5 µg of biotinylated goat anti-rat Type IV Collagen antibody or biotinylated goat IgG isotype control antibody (SouthernBiotech, Birmingham, AL, USA) was added to per $10^8$ MBs. After incubation for 30 min at room temperature, MB$_{Col IV}$ or isotype control MBs (MB$_{Ctrl}$) were collected by centrifugation.

Non-targeted MBs ($MB_N$) without conjugated primary antibody were also prepared.

## Characterization of MBs

To confirm the conjugation of Type IV Collagen antibody to the surface of MBs, Alexa Fluor® 555-labeled anti-goat secondary antibody (Invitrogen, Carlsbad, CA, USA) was added to $MB_{Col\,IV}$ and mixed for 30 min at room temperature. The mixture was separated by centrifugation and the upper layer was washed twice with PBS to eliminate the free secondary antibody. The fluorescence-labeled $MB_{Col\,IV}$ were examined by a fluorescence inversion microscopy (Olympus Corporation, Tokyo, Japan).

To analyze the characteristics of the $MB_{Col\,IV}$, $MB_N$ were used as the blank control. The morphology of the MBs were examined by using bright-field and fluorescence inversion microscopy (Olympus Corporation, Tokyo, Japan). Particle size, size distribution and concentration of MBs were determined by using the Accusizer 780 Optical Particle Sizer (Particle Sizing Systems, Santa Barbara, CA, USA) with a 0.5 μm diameter detection limit.

## Carotid Artery Injury Model

All animal procedures were performed in accordance with the principles outlined in the Guide for the Care and Use of Laboratory Animals and approved by Animal Care and Use Committee. Adult male Sprague–Dawley rats (Vital River Laboratory, Beijing, China), weighing 400–500 g, underwent the rat carotid artery balloon injury as previously described (Chan et al., 2011; Petrasheskaya et al., 2016). Rats were given aspirin by oral gavage before surgery and kept anesthetized by isoflurane at 2% at 2 L/min oxygen. Following a midline neck incision, the left common carotid artery (LCCA), left external carotid artery (LECA), and left internal carotid artery (LICA) were exposed. After distal ligation of the LECA, the proximal end of LCCA and the distal end of LICA were then temporarily clipped by arterial clamps and a 2-French arterial embolectomy catheter (Edwards Lifesciences, Irvine, CA, USA) was advanced proximally into LCCA through the incision of LECA. The balloon was inflated and withdrawn with a rotating action to the arteriotomy in LECA and then reintroduced and retracted twice again. The balloon catheter was removed and the LECA was ligated. Finally, arterial clamps were removed to restore the blood flow, and then the neck incision was closed. Thereafter, rat carotid artery injury model was performed and used for the following experiments.

## Histological Analysis

Bilateral carotid arteries were harvested following *in situ* perfusion fixation with PBS and 4% paraformaldehyde. Tissues were placed in paraformaldehyde for 1 h at 4°C, then overnight in 30% sucrose in PBS at 4°C for cryo-protection. Vessels were coated with Optimum Cutting Temperature O.C.T.™ compound (Tissue Tek, Hatfield, PA) and transferred to liquid nitrogen for flash-freeze. Vessels were sectioned to obtain arterial cross-sections across the length of the artery by cryostat microtome (CM1950; Leica, Heidelberg, Germany) and were examined histologically using routine hematoxylin-eosin (H&E) staining for morphometric analysis. Digital images were

collected with bright-field by inversion microscopy (Olympus Corporation, Tokyo, Japan).

## *Ex vivo* Adhesion of MBs

Attachment ability of MBs to collagen IV was evaluated by counting the number of adhering MBs. Briefly, after the rat carotid artery injury model and the *in situ* perfusion fixation were completed, the LCCA was harvested and then opened longitudinally. The side of adventitia was adhered to a coverslip. Then MBs were added into a 6-well plate ($2 \times 10^7$ MBs per well) and filled with PBS. Due to the static flotation nature of MBs, the coverslip with the artery coated faced downward to maximize interaction between the tissue and MBs for 5 min at room temperature. After that, the free MBs were removed by rinsing five times with PBS. To further determine the specificity of MBs adhesion, vessel tissues were pretreated with 25 μg/mL goat anti-rat Type IV Collagen antibody to block available receptors prior to $MB_{Col\,IV}$ incubation. Digital images were obtained with bright-field by inversion microscopy (Olympus Corporation, Tokyo, Japan) to count the number of attached MBs in five random fields of view.
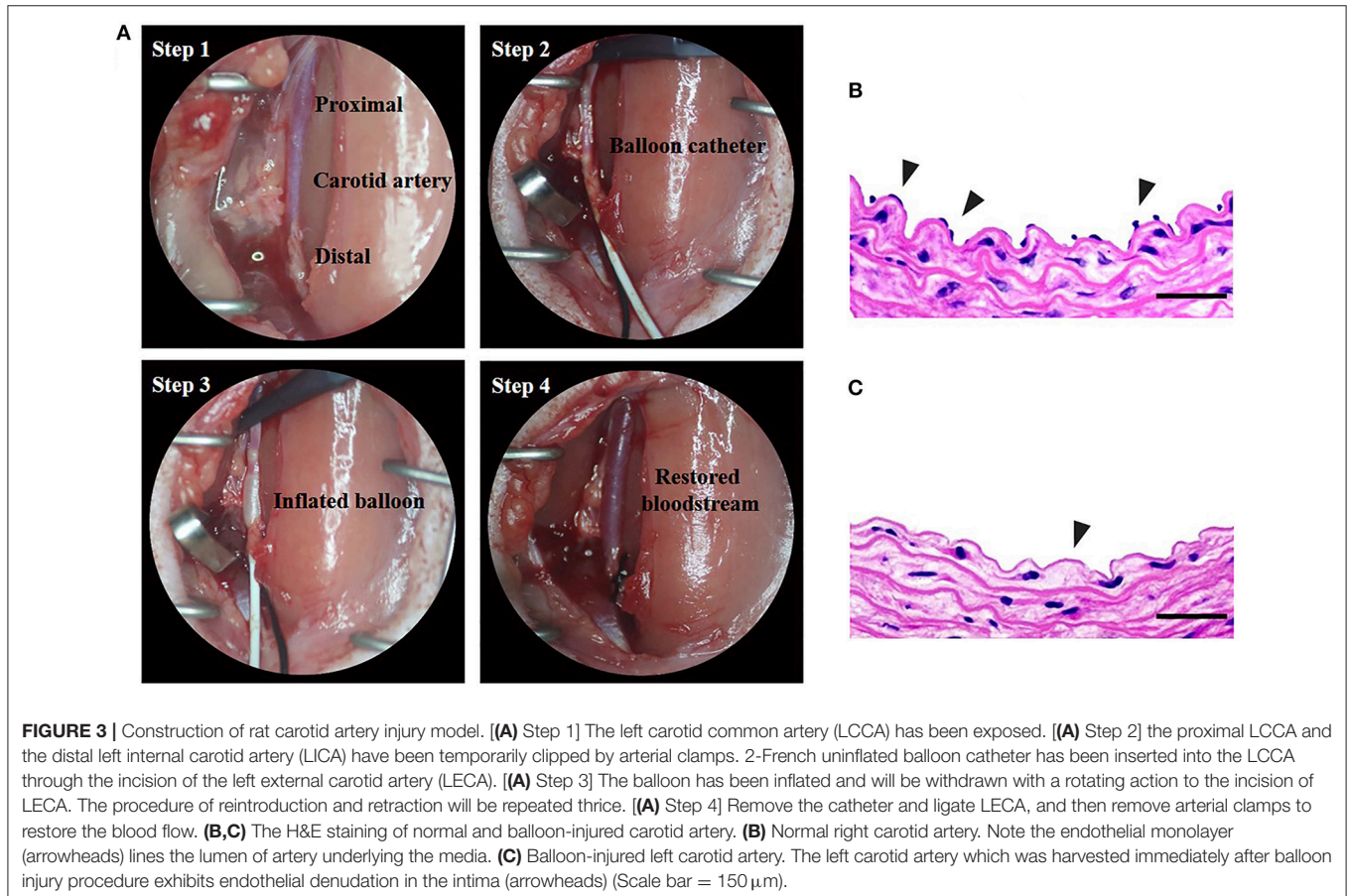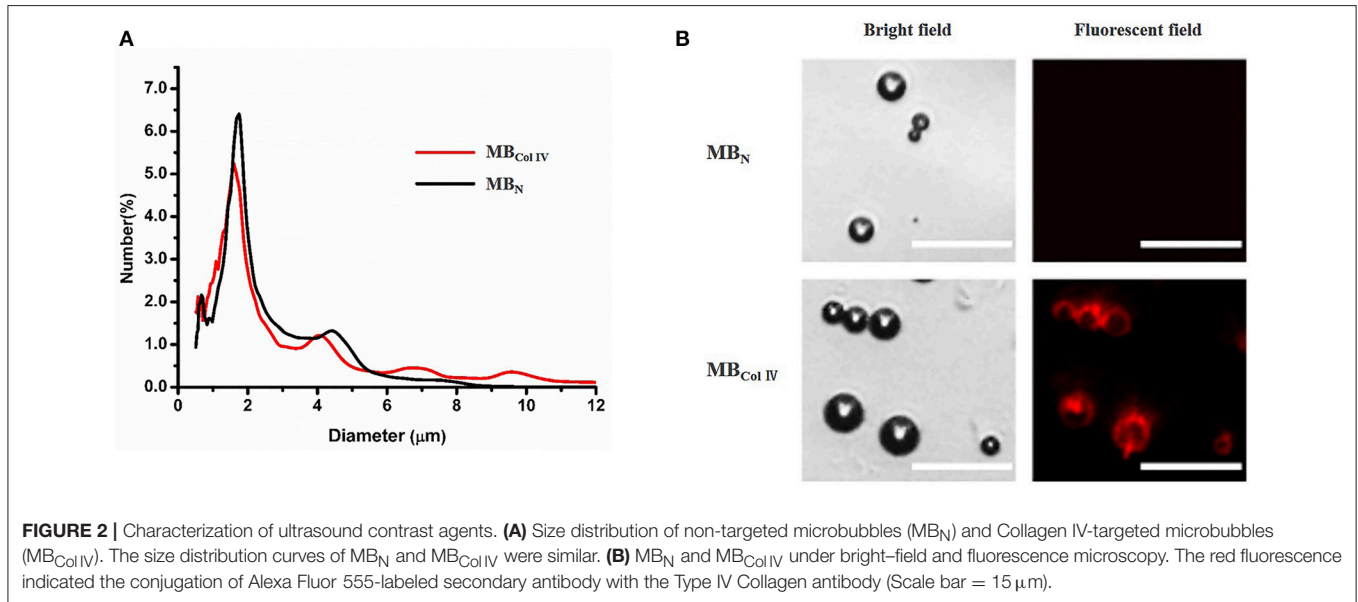
## *In vivo* Ultrasound Molecular Imaging

After rat carotid artery injury model was developed as described above, rats were kept anesthetized on a heated stage throughout the imaging session. Ultrasound molecular imaging was performed with a commercial ultrasound system Resona 7 (Mindray Medical Systems, Shenzhen, China) using a L11-3 linear array transducer. Contrast imaging mode was applied in the ultrasound molecular imaging experiments. All imaging parameters were kept constant throughout the whole procedure as follows: frequency 5.6 MHz, depth 2 cm, gain 45 dB, frame rate 10 Hz, dynamic range 115 dB, and mechanical index 0.085. In order to reduce motion interference, both the transducer and the rats were fixed to maintain the same long axis cross section of carotid artery. The concentration of MBs suspension was adjusted to $2 \times 10^8$ MBs/ml. Then 200 μl MBs suspension was injected intravenously through tail vein following by flushing with 50 μl PBS. Four minutes after MBs injection, 100 frames of images were captured to obtain a signal from adherent and freely circulating MBs. A continuous high-power destructive pulse (mechanical index: 0.553) was then applied for 2 s to destroy these MBs. After 2 s, to allow the freely circulating MBs to replenish, another 100 frames of images were acquired, in which the ultrasonic signals were from any residual freely circulating MBs and tissue. To minimize the bias and test the specificity of these molecular imaging signals only resulting from adherent targeted MBs, $MB_{ColIV}$, and $MB_{Ctrl}$ were administered in random order to all rats. Another 30-min delay was allowed to clear MBs from the preceding imaging session. As a control, ultrasound molecular imaging was also performed in normal rats to further assess the specificity of MBs adhesion. The acoustic imaging signals were analyzed by using commercially available analysis software (Mindray Medical Systems, Shenzhen, China). As previously described (Wu et al., 2011), the difference in signal intensity from adherent MBs was calculated by subtracting the post-destruction signal from the pre-destruction signal.

## Immunohistochemistry

Immunostaining analysis for collagen IV was performed to confirm that collagen IV was exposed through endothelium denudation. Briefly, LCCAs from normal artery group and balloon-injured artery group were excised, followed by *in situ* perfusion fixation with PBS and 4% paraformaldehyde. Then artery samples were transferred to paraformaldehyde overnight, followed by ethanol dehydration and paraffin



**FIGURE 2 |** Characterization of ultrasound contrast agents. **(A)** Size distribution of non-targeted microbubbles (MB$_N$) and Collagen IV-targeted microbubbles (MB$_{Col IV}$). The size distribution curves of MB$_N$ and MB$_{Col IV}$ were similar. **(B)** MB$_N$ and MB$_{Col IV}$ under bright–field and fluorescence microscopy. The red fluorescence indicated the conjugation of Alexa Fluor 555-labeled secondary antibody with the Type IV Collagen antibody (Scale bar = 15 μm).



**FIGURE 3 |** Construction of rat carotid artery injury model. [**(A)** Step 1] The left carotid common artery (LCCA) has been exposed. [**(A)** Step 2] the proximal LCCA and the distal left internal carotid artery (LICA) have been temporarily clipped by arterial clamps. 2-French uninflated balloon catheter has been inserted into the LCCA through the incision of the left external carotid artery (LECA). [**(A)** Step 3] The balloon has been inflated and will be withdrawn with a rotating action to the incision of LECA. The procedure of reintroduction and retraction will be repeated thrice. [**(A)** Step 4] Remove the catheter and ligate LECA, and then remove arterial clamps to restore the blood flow. **(B,C)** The H&E staining of normal and balloon-injured carotid artery. **(B)** Normal right carotid artery. Note the endothelial monolayer (arrowheads) lines the lumen of artery underlying the media. **(C)** Balloon-injured left carotid artery. The left carotid artery which was harvested immediately after balloon injury procedure exhibits endothelial denudation in the intima (arrowheads) (Scale bar = 150 μm).

embedment. Artery samples were sectioned to obtain arterial cross-sections. After the process of deparaffinage and rehydration, slides were blocked and then incubated with the primary antibody goat anti-rat Type IV Collagen (SouthernBiotech, Birmingham, AL, USA), followed by being rinsed with PBS thrice and then incubated with horseradish peroxidase-conjugated secondary antibodies. Finally, slides were incubated with diaminobenzidine for horseradish peroxidase reaction. In order to exhibit the tissue morphology of vascular wall, slides were counterstained with hematoxylin. Immunohistochemical images were acquired by using inversion microscopy (Olympus Corporation, Tokyo, Japan) under bright field.

## Statistical Analysis

Data were analyzed by the statistic software SPSS 20.0 (IBM Corp, Armonk, New York, USA). As values were normally distributed, statistic difference between two groups was determined by Student's $t$-test, and one-way ANOVA were used to compare among more than two groups. If the differences among these groups were significant for one-way ANOVA, the difference between the two groups was conducted by Student-Newman-Keuls test. The $P < 0.05$ indicated statistically significant difference.
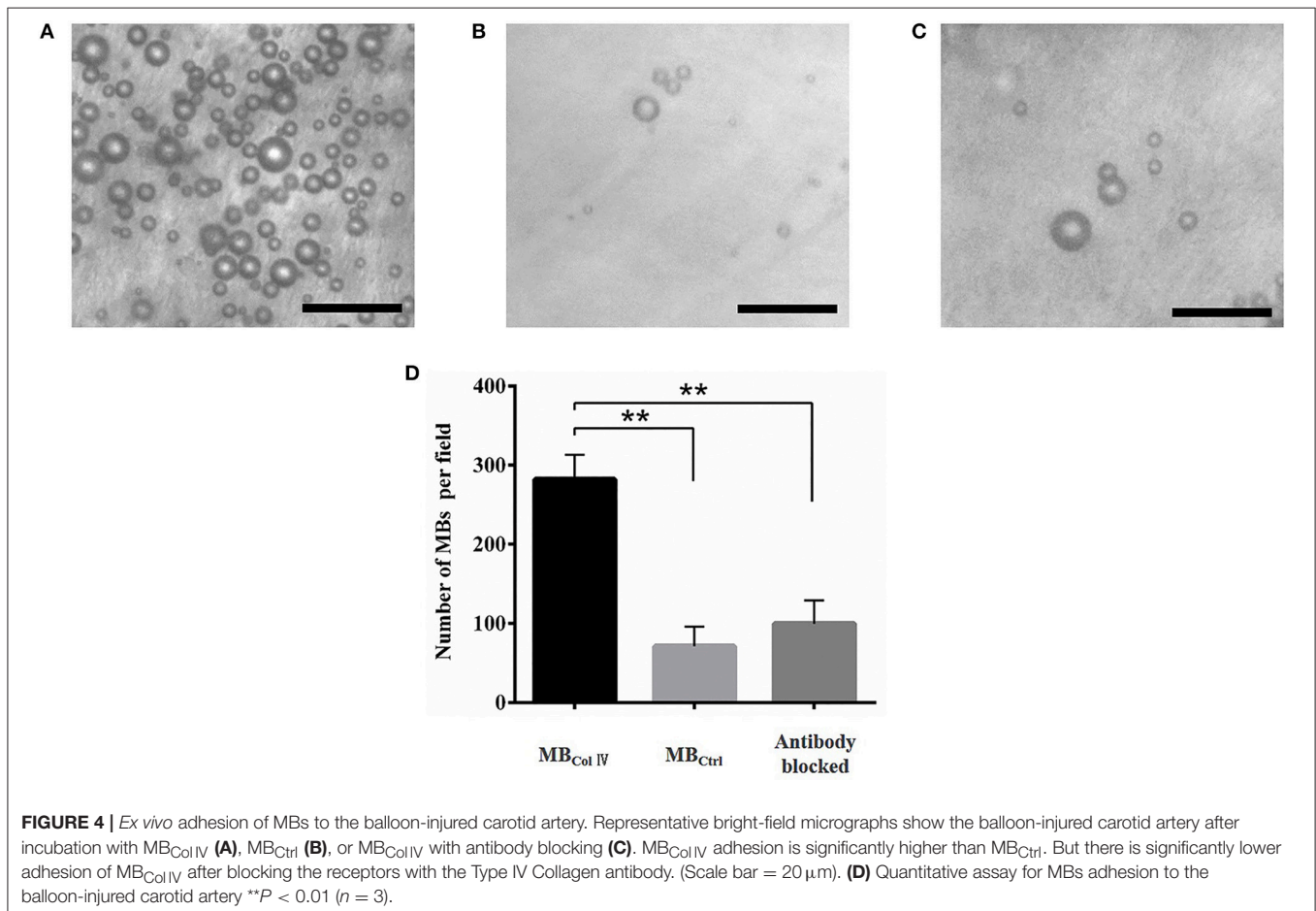
## RESULTS

### Characteristics of MBs

The fabricated $MB_{Col\,IV}$ appeared a typical multi-peak particle distribution. There was no significant difference between $MB_{Col\,IV}$ and $MB_N$ for the particle size and distribution (all $P > 0.05$). The mean diameter of $MB_{Col\,IV}$ and $MB_N$ were 1.92 and 1.89 $\mu$m, respectively. The results demonstrated that the conjunction of avidin and biotinylated antibody to MBs surface did not change the particle size and distribution of MBs (**Figure 2A**). **Figure 2B** showed that both $MB_{Col\,IV}$ and $MB_N$ had smooth and spherical morphology for microscopic observation. The surface of $MB_{Col\,IV}$ emitted a bright red fluorescence, indicating the anti-rat Type IV Collagen antibodies were successfully conjugated onto the surface of these MBs (**Figure 2B**).

### Confirmation of Rat Carotid Artery Injury

Vascular balloon injury is a standardized protocol for endothelial denudation and intimal damage through repeated insertion and retreat of the balloon catheter (**Figure 3A**). In order to confirm the successful development of carotid artery injury model, cross-sections were stained with H&E. From the **Figures 3B,C** we can see that LCCA lost an endothelial monolayer after vascular



**FIGURE 4** | *Ex vivo* adhesion of MBs to the balloon-injured carotid artery. Representative bright-field micrographs show the balloon-injured carotid artery after incubation with $MB_{Col\,IV}$ **(A)**, $MB_{Ctrl}$ **(B)**, or $MB_{Col\,IV}$ with antibody blocking **(C)**. $MB_{Col\,IV}$ adhesion is significantly higher than $MB_{Ctrl}$. But there is significantly lower adhesion of $MB_{Col\,IV}$ after blocking the receptors with the Type IV Collagen antibody. (Scale bar = 20 $\mu$m). **(D)** Quantitative assay for MBs adhesion to the balloon-injured carotid artery **$P < 0.01$ ($n = 3$).
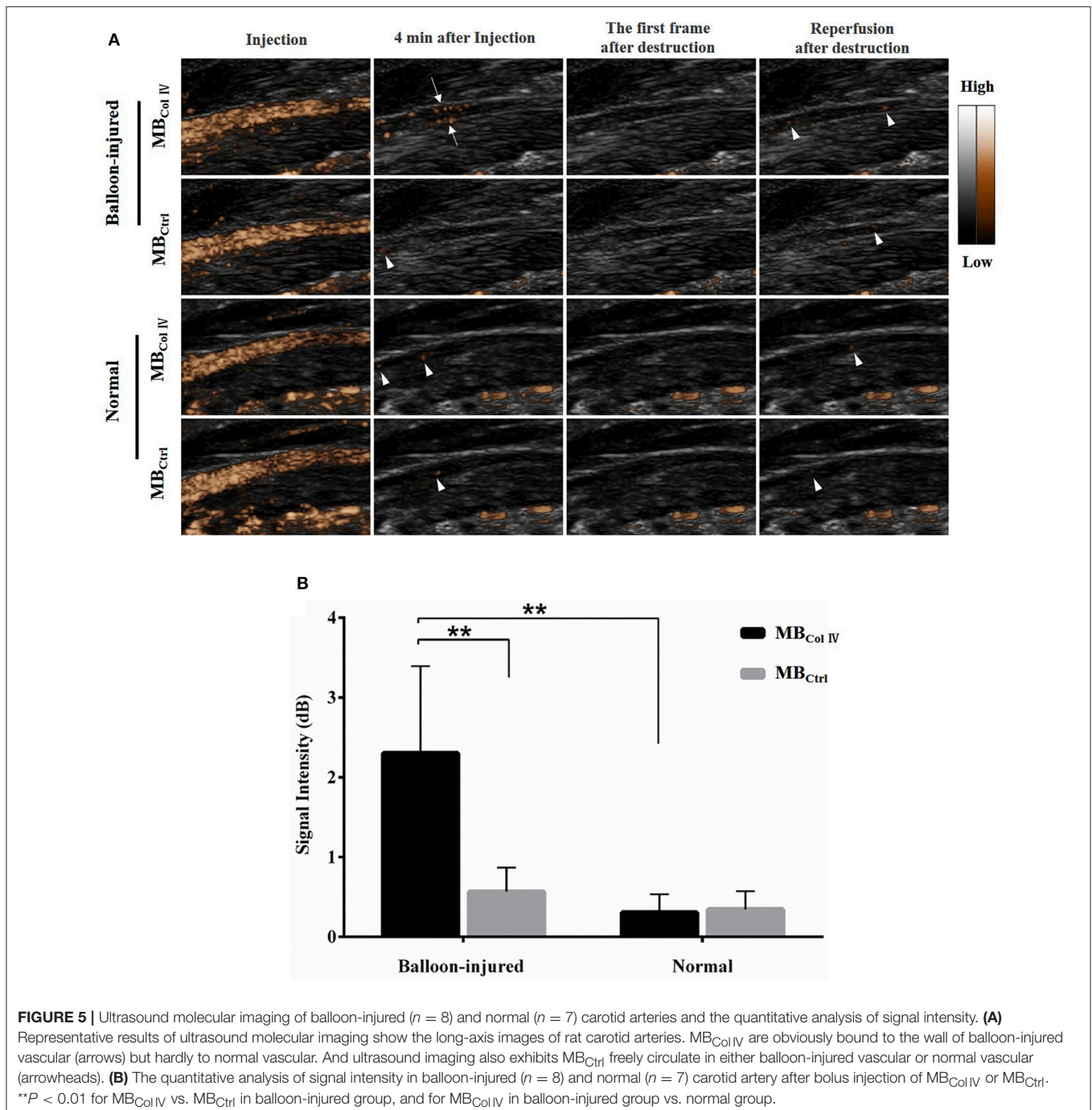
balloon injury, compared with the normal right common carotid artery (RCCA). The results showed that we successfully constructed the carotid injury model.

## Binding Specificity of MBs *ex vivo*
To determine the binding specificity of $MB_{Col IV}$, we performed the binding specificity experiments *ex vivo* through incubating the $MB_{Col IV}$ or $MB_{Ctrl}$ with the injured LCCA. After a static exposure of the injured LCCA to MBs, we could see that a large number of $MB_{Col IV}$ were adhered to the injured vessel (**Figure 4A**), which was significantly higher than $MB_{Ctrl}$ (**Figure 4B**). Meanwhile, pre-blocking receptors in injured LCCA by anti-rat Type IV Collagen antibodies greatly reduced the attachment of $MB_{Col IV}$ (**Figure 4C**). Quantitative analysis indicated that the binding efficiency of $MB_{Col IV}$ was about four times higher compared with $MB_{Ctrl}$ (282.1 $\pm$ 77.2 MBs per field vs. 71.07 $\pm$ 62.07 per field, $P < 0.01$) (**Figure 4D**).



**FIGURE 5 |** Ultrasound molecular imaging of balloon-injured ($n = 8$) and normal ($n = 7$) carotid arteries and the quantitative analysis of signal intensity. **(A)** Representative results of ultrasound molecular imaging show the long-axis images of rat carotid arteries. $MB_{Col IV}$ are obviously bound to the wall of balloon-injured vascular (arrows) but hardly to normal vascular. And ultrasound imaging also exhibits $MB_{Ctrl}$ freely circulate in either balloon-injured vascular or normal vascular (arrowheads). **(B)** The quantitative analysis of signal intensity in balloon-injured ($n = 8$) and normal ($n = 7$) carotid artery after bolus injection of $MB_{Col IV}$ or $MB_{Ctrl}$. **P < 0.01 for $MB_{Col IV}$ vs. $MB_{Ctrl}$ in balloon-injured group, and for $MB_{Col IV}$ in balloon-injured group vs. normal group.

## Ultrasound Molecular Imaging

To further evaluate the special adherence of MBs and their ultrasound imaging effect *in vivo*, ultrasound molecular imaging was performed in the balloon-injured carotid artery group ($n = 8$) and the normal carotid artery group ($n = 7$). As shown in **Figure 5A**, 4 min after MBs injection, almost all of MBs had been washed out. Meanwhile, $MB_{Col\,IV}$ were hardly attached to the normal artery wall (**Figure 5A**). By contrast, $MB_{Col\,IV}$ were obviously adhered to the inner wall of balloon-injured artery (**Figure 5A** and Supplementary Video 1). After the trigger of the destruction pulse, no echo signal of MBs was found in balloon-injured the carotid artery group and the normal carotid artery group (**Figure 5A**). This procedure further confirmed that $MB_{Col\,IV}$ were attached to the inner vessel wall. Quantitative analysis revealed that the signal intensity of $MB_{Col\,IV}$ ($2.30 \pm 0.91$ dB) was higher than $MB_{Ctrl}$ ($0.57 \pm 0.26$ dB) in balloon-injured carotid artery group ($P < 0.01$) (**Figure 5B**). Moreover, the signal intensity of $MB_{Col\,IV}$ in the balloon-injured carotid artery group was also significantly higher than normal carotid artery group ($2.30 \pm 0.91$ dB vs. $0.31 \pm 0.21$ dB, $P < 0.01$) (**Figure 5B**).
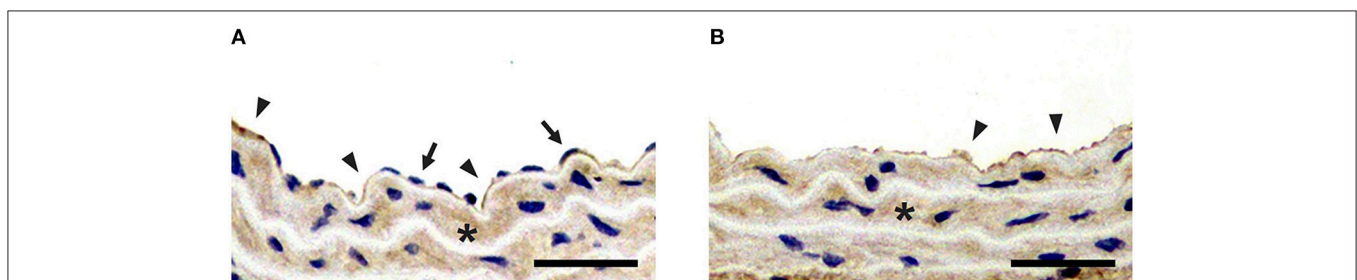
## Immunohistochemistry

To confirm the results of ultrasound molecular imaging, LCCAs of the normal group and balloon-injured group were harvested and analyzed for the exposure of collagen IV after endothelium denudation. The results of immunohistochemical staining examination were presented in **Figure 6**. We could see that both balloon-injured artery and normal artery were stained dark brown for collagen IV in basement membrane, indicating collagen IV was a major constituent of the basement membrane. It was consistent with the previous studies (Kalluri, 2003; Abreu-Velez and Howard, 2012; Manon-Jensen et al., 2016). In normal artery intima, collagen IV presenting in basement membrane, was covered by a monolayer endothelium (**Figure 6A**). However, without endothelium coverage, collagen IV was directly exposed in balloon-injured artery (**Figure 6B**). The exposure of collagen IV greatly enhanced the interaction opportunity with $MB_{Col\,IV}$. In addition, collagen IV was also a component of the basement membrane for SMCs in tunica media, which had been reported in previous studies (Shekhonin et al., 1985; Howard and Macarak, 1989).

## DISCUSSION

Microbubble-based ultrasound molecular imaging is a promising approach in the disease diagnosis at the early stage. This is especially the case for vascular disorders since the microscale-targeted bubbles only exist in the blood and are not extravasate from the circulation. This feature makes it greatly standing out from other nanoparticle-based molecular imaging modalities, such as quantum dot-based optical molecular imaging and iron nanoparticle-based magnetic imaging resonance (Lobatto et al., 2011). Moreover, ultrasound is a safe, affordable and real-time imaging modality and can detect deep-seated diseased tissues. All of these features of ultrasound prompted us to explore the diagnosis feasibility of injured artery by using ultrasound molecular imaging.

In our study, we fabricated the targeted $MB_{Col\,IV}$ by biotin-avidin bridging method. As shown in **Figure 2B**, collagen IV antibodies were successfully conjugated to the surface of MBs. It has to be pointed out that we did not use the *in vitro* tool in our static binding experiments such as culture plates, pre-coated with Matrigel, which has been taken to examine the binding of targeted particles to collagen IV (Dong et al., 2016). In fact, they are not suitable in our experiments. Due to the Matrigel's water solubility, Matrigel dissolves in PBS during rinsing, and almost all MBs would be washed away (data not shown). Therefore, we used the harvested tissue of injured carotid artery to examine the affinity effect of MBs. Effective and special targeting affinity was achieved in our *ex vivo* binding experiments (**Figure 4**). The number of $MB_{Col\,IV}$ binding to the tissue of injured artery was nearly four times higher than $MB_{Ctrl}$, indicating $MB_{Col\,IV}$ we obtained can be used as a potential ultrasound molecular imaging probe.

In our present study, we used intravenously injection for ultrasound molecular imaging *in vivo* in order to determine whether $MB_{Col\,IV}$ could adhere to the site of endothelial denudation and be visually detected by a clinical ultrasound scanner or not. Surprisingly, we found stronger ultrasound molecular imaging signals from injured vascular wall after $MB_{Col\,IV}$ injection but not $MB_{Ctrl}$, the former being nearly five times higher than $MB_{Ctrl}$. Interestingly, no obvious ultrasound molecular imaging signals were detected from the normal



**FIGURE 6 |** Immunohistochemical staining for collagen IV. **(A)** Immunohistochemical staining of the left carotid common artery (LCCA) from normal group. **(B)** Immunohistochemical staining of LCCA from balloon-injured group. Positive staining for collagen IV is presented in both normal and balloon-injured artery (brown stain; arrowheads). Compared with the endothelium (arrows) coverage for collagen IV (arrowheads) in normal artery, collagen IV is exposed after endothelium denudation in balloon-injured artery (arrowheads). Besides, Collagen IV is also localized to tunica media (asterisk) (Scale bar = 150 μm).

arterial wall after MB$_{Col IV}$ or MB$_{Ctrl}$ injection. These results suggested that MB$_{Col IV}$ had a highly specific binding ability to these collagen IV targets and could function as an ultrasound molecular imaging probe to detect vascular injury. To take the drug-loaded advantages of MBs into consideration, it is easy to design the MB$_{Col IV}$ into drug-loaded targeted MBs through carrying drugs (Lammertink et al., 2015), gene (Zhao et al., 2018) and/or especially therapeutic gas, such as nitric oxide, hydrogen sulfide, carbon monoxide, and so on (Fix et al., 2015). If that is the case, we have reasons to believe that MB$_{Col IV}$ could be further functionalized as theranostics agent and would play a great role for ultrasound imaging-guided treatment of vascular injury.

There are several limitations in our study. The rat carotid artery balloon injury model described in our study imitate vascular injury by angioplasty. However, in clinical practice, restenosis occurs in patients who have occlusive atherosclerotic lesions after dilating the narrow lumen through angioplasty. Besides, to evaluate non-culprit stenosis severity, the instantaneous wave-free ratio, which is helpful for guiding PCI strategy, has been regarded as the promising method and used in patients with acute coronary syndrome and multivessel disease (Indolfi et al., 2015). In order to reduce complications, coronary balloon angioplasty is usually combined with stent implantation during PCI (Byrne et al., 2017). Compared with human angioplasty, the rat carotid artery balloon injury model is lacking atherosclerotic lesions and stent implantation. Whereas, the above artery injury model is widely perceived as a well-defined model for researching vascular remodeling and vascular cell proliferation, and it is only suitable for the proof-of-concept study. Another limitation is that once the collagen underlying the basement membrane is exposed, it may cause thrombogenesis, producing an obstruction for targeted MBs. To prevent thrombogenesis, an anticoagulant drug is used before balloon manipulation, but this procedure does not affect the prognosis of restenosis model (Chan et al., 2011; Riegler et al., 2013). Furthermore, the method of avidin-biotin linkage is unlikely to be applied in human clinical practice because of the potential immune response. Therefore, a covalent linkage method is expected to be used to develop targeted contrast agents in the future. For instance, small molecules such as biotin and peptides can be attached to the shell-forming material (protein or lipid) before bubble generation (Weinkauf et al., 2018).

In summary, we have successfully fabricated MB$_{Col IV}$ by conjugating anti-collagen IV antibodies to the surface of MBs and confirmed the feasibility to apply them for ultrasound molecular imaging of endothelial injury at early stage. Our study provides an early diagnosis tool for restenosis due to endothelial damage and a potential platform for image-guided therapy for vascular injury.

## AUTHOR CONTRIBUTIONS

XM and BZ initialed the project. XM and FY conducted the experiment and data analysis. BZ and FY provided equipment, materials, and experimental methods. XM wrote the manuscript. FY proofread the manuscript. All authors agreed with the final version of the manuscript.

## FUNDING

## ACKNOWLEDGMENTS

## REFERENCES

Abreu-Velez, A., and Howard, M. (2012). Collagen IV in normal skin and in pathological processes. *N. Am. J. Med. Sci.* 4, 1–8. doi: 10.4103/1947-2714.92892

Amsterdam, E. A., Wenger, N. K., Brindis, R. G., Casey, D. E. Jr., Ganiats, T. G., Holmes, D. R. Jr., et al. (2014). 2014 AHA/ACC guideline for the management of patients with non-ST-elevation acute coronary syndromes: a report of the american college of cardiology/american heart association task force on practice guidelines. *J. Am. Coll. Cardiol.* 64, e139–e228. doi: 10.1016/j.jacc.2014.09.017

Bavry, A. A., Kumbhani, D. J., Rassi, A. N., Bhatt, D. L., and Askari, A. T. (2006). Benefit of early invasive therapy in acute coronary syndromes: a meta-analysis of contemporary randomized clinical trials. *J. Am. Coll. Cardiol.* 48, 1319–1325. doi: 10.1016/j.jacc.2006.06.050

Byrne, R. A., Stone, G. W., Ormiston, J., and Kastrati, A. (2017). Coronary balloon angioplasty, stents, and scaffolds. *Lancet* 390, 781–92. doi: 10.1016/S0140-6736(17)31927-X

Chan, J. M., Rhee, J. W., Drum, C. L., Bronson, R. T., and Golomb, G. (2011). *In vivo* prevention of arterial restenosis with paclitaxel-encapsulated targeted lipid–polymeric nanoparticles. *Proc. Natl. Acad. Sci. U.S.A.* 108, 19347–52. doi: 10.1073/pnas.1115945108

Davis, C., Fischer, J., Ley, K., and Sarembock, I. J. (2003). The role of inflammation in vascular injury and repair. *J. Thromb. Haemost.* 1, 1699–709. doi: 10.1046/j.1538-7836.2003.00292.x

Deshpande, N., Pysz, M. A., and Willmann, J. K. (2010). Molecular ultrasound assessment of tumor angiogenesis. *Angiogenesis* 13, 175–188. doi: 10.1007/s10456-010-9175-z

Dong, Y., Chen, H., Chen, C., Zhang, X., Tian, X., Zhang, Y., et al. (2016). Polymer-lipid hybrid theranostic nanoparticles co-delivering ultrasmall superparamagnetic iron oxide and paclitaxel for targeted magnetic resonance imaging and therapy in atherosclerotic plaque. *J. Biomed. Nanotechnol.* 12, 1245–1257. doi: 10.1166/jbn.2016.2239

Fix, S. M., Borden, M. A., and Dayton, P. A. (2015). Therapeutic gas delivery via microbubbles and liposomes. *J. Control. Release* 209, 139–149. doi: 10.1016/j.jconrel.2015.04.027

Howard, P. S., and Macarak, E. J. (1989). Localization of collagen types in regional segments of the fetal bovine aorta. *Lab. Invest.* 61, 548–555.

Indolfi, C., Mongiardo, A., Spaccarotella, C., Torella, D., Caiazzo, G., Polimeni, A., et al. (2015). The instantaneous wave-free ratio (iFR) for evaluation of

non-culprit lesions in patients with acute coronary syndrome and multivessel disease. *Int. J. Cardiol.* 178, 46–54. doi: 10.1016/j.ijcard.2014.03.210

Kalluri, R. (2003). Basement membranes: structure, assembly and role in tumour angiogenesis. *Nat. Rev. Cancer* 3, 422–433. doi: 10.1038/nrc1094

Kennedy, S., McPhaden, A. R., Wadsworth, R. M., and Wainwright, C. L. (2000). Correlation of leukocyte adhesiveness, adhesion molecule expression and leukocyte-induced contraction following balloon angioplasty. *Br. J. Pharmacol.* 130, 95–103. doi: 10.1038/sj.bjp.0703282

Lammertink, B. H., Bos, C., Deckers, R., Storm, G., Moonen, C. T. W., and Escoffre, J.-M. (2015). Sonochemotherapy: from bench to bedside. *Front. Pharmacol.* 6:138. doi: 10.3389/fphar.2015.00138

Leong-Poi, H. (2009). Molecular imaging using contrast-enhanced ultrasound: evaluation of angiogenesis and cell therapy. *Cardiovasc. Res.* 84, 190–200. doi: 10.1093/cvr/cvp248

Lindner, J. R. (2009). Contrast ultrasound molecular imaging of inflammation in cardiovascular disease. *Cardiovasc. Res.* 84, 182–189. doi: 10.1093/cvr/cvp302

Lobatto, M. E., Fuster, V., Fayad, Z. A., and Mulder, W. J. (2011). Perspectives and opportunities for nanomedicine in the management of atherosclerosis. *Nat. Rev. Drug Discov.* 10, 835–852. doi: 10.1038/nrd3578

Manon-Jensen, T., Kjeld, N. G., and Karsdal, M. A. (2016). Collagen-mediated hemostasis. *J. Thromb. Haemost.* 14, 438–448. doi: 10.1111/jth.13249

Meyers, M. W., Rink, J. S., Jiang, Q., Kelly, M. E., Vercammen, J. M., Thaxton, C. S., et al. (2017). Systemically administered collagen-targeted gold nanoparticles bind to arterial injury following vascular interventions. *Physiol. Rep.* 5:e13128. doi: 10.14814/phy2

Murray, C. J., Vos, T., Lozano, R., Naghavi, M., Flaxman, A. D., Michaud, C., et al. (2012). Disability-adjusted life years (DALYs) for 291 diseases and injuries in 21 regions, 1990-2010: a systematic analysis for the Global Burden of Disease Study 2010. *Lancet* 380, 2197–2223. doi: 10.1016/S0140-6736(12)61689-4

Otsuka, F., Yasuda, S., Noguchi, T., and Ishibashi-Ueda, H. (2016). Pathology of coronary atherosclerosis and thrombosis. *Cardiovasc. Diagn. Ther.* 6, 396–408. doi: 10.21037/cdt.2016.06.01

Petrasheskaya, N., Tae, H.-J., Ahmet, I., Talan, M. I., Lakatta, E. G., and Lin, L. (2016). A rat carotid balloon injury model to test anti-vascular remodeling therapeutics. *J. Vis. Exp.* 2016:e53777. doi: 10.3791/53777

Riegler, J., Liew, A., Hynes, S. O., Ortega, D, o'Brien, T., Day, R. M., et al. (2013). Superparamagnetic iron oxide nanoparticle targeting of MSCs in vascular injury. *Biomaterials* 34, 1987–1994. doi: 10.1016/j.biomaterials.2012.11.040

Shekhonin, B. V., Domogatsky, S. P., Muzykantov, V. R., Idelson, G. L., and Rukosuev, V. S. (1985). Distribution of type I, III, IV and V collagen in normal and atherosclerotic human arterial wall: immunomorphological characteristics. *Coll. Relat. Res.* 5, 355–368.

Tanaka, H., Sukhova, G. K., Swanson, S. J., Clinton, S. K., Ganz, P., Cybulsky, M. I., et al. (1993). Sustained activation of vascular cells and leukocytes in the rabbit aorta after balloon injury. *Circulation* 88, 1788–1803.

Villanueva, F. S., and Wagner, W. R. (2008). Ultrasound molecular imaging of cardiovascular disease. *Nat. Clin. Pract. Cardiovasc. Med.* 5(Suppl. 2), S26–S32. doi: 10.1038/ncpcardio1246

Weinkauf, C. C., Concha-Moore, K., Lindner, J. R., Marinelli, E. R., Hadinger, K. P., Bhattacharjee, S., et al. (2018). Endothelial vascular cell adhesion molecule 1 is a marker for high-risk carotid plaques and target for ultrasound molecular imaging. *J. Vasc. Surg.* 68, 105S−113S. doi: 10.1016/j.jvs.2017.10.088

Willmann, J. K., Paulmurugan, R., Chen, K., Gheysens, O., Rodriguez-Porcel, M., Lutz, A. M., et al. (2008). US imaging of tumor angiogenesis with microbubbles targeted to vascular endothelial growth factor receptor type 2 in mice. *Radiology* 246, 508–518. doi: 10.1148/radiol.2462070536

Wu, J., Leong-Poi, H., Bin, J., Yang, L., Liao, Y., Liu, Y., et al. (2011). Efficacy of contrast-enhanced US and magnetic microbubbles targeted to vascular cell adhesion molecule-1 for molecular imaging of atherosclerosis. *Radiology* 260, 463–471. doi: 10.1148/radiol.11102251

Yan, F., Li, L., Deng, Z., Jin, Q., Chen, J., Yang, W., et al. (2013). Paclitaxel-liposome-microbubble complexes as ultrasound-triggered therapeutic drug delivery carriers. *J. Control. Release* 166, 246–255. doi: 10.1016/j.jconrel.2012.12.025

Yan, F., Sun, Y., Mao, Y., Wu, M., Deng, Z., Li, S., et al. (2018). Ultrasound molecular imaging of atherosclerosis for early diagnosis and therapeutic evaluation through leucocyte-like multiple targeted microbubbles. *Theranostics* 8, 1879–1891. doi: 10.7150/thno.22070

Zhao, R., Liang, X., Zhao, B., Chen, M., Liu, R., Sun, S., et al. (2018). Ultrasound assisted gene and photodynamic synergistic therapy with multifunctional FOXA1-siRNA loaded porphyrin microbubbles for enhancing therapeutic efficacy for breast cancer. *Biomaterials* 173, 58–70. doi: 10.1016/j.biomaterials.2018.04.054

**Conflict of Interest Statement:** The authors declare that the research was conducted in the absence of any commercial or financial relationships that could be construed as a potential conflict of interest.